Measuring the impact of urban morphology on residential energy consumption at the neighborhood-level in the Netherlands

Yu, H.; Hu, M.; Tukker, A.; Berrill, P.

Sustainable Cities and Society 145 (2026) 107449

Contents lists available at ScienceDirect

Sustainable Cities and Society

journal homepage: www.elsevier.com/locate/scs

Measuring the impact of urban morphology on residential energy consumption at the neighborhood-level in the Netherlands

Han Yu [a,*], Mingming Hu [a], Arnold Tukker [a,b], Peter Berrill [a]

[a] Institute of Environmental Sciences (CML), Leiden University, P.O. Box 9518, Leiden 2300 RA, the Netherlands
[b] Netherlands Organization for Applied Scientific Research TNO, the Netherlands

ARTICLE INFO

Keywords:
Urban morphology
Spatial Durbin Model
Residential energy consumption
Neighborhood scale
Heating-dominated climates

ABSTRACT

In the Netherlands, the residential sector accounted for 16.8% of total final energy consumption in 2022, mostly from natural gas. Current policies and standards aimed at reducing residential energy consumption mainly focus on improving the performance of buildings and appliances. Previous studies on urban heat island effects have consistently shown that urban areas tend to be warmer than their surroundings, while some have further highlighted that spatial arrangements of land use types can moderate local microclimatic conditions, which may in turn influence local energy consumption. However, assessments of the impacts of urban morphology on residential energy consumption remain limited, especially for space heating demands in winter. In this study, we develop a systematic framework to define and classify urban morphology indicators at the neighborhood scale. We apply this framework to neighborhoods in the Netherlands and employ a Spatial Durbin Model to estimate the impacts of urban morphology on per-capita residential energy consumption (REPC), considering landscape metrics, building characteristics, and demographic indicators under the broader definition of urban morphology. The results reveal that more compact built environments and interspersed water bodies are associated with lower REPC, whereas tree- and grass-covered green infrastructure show mutually opposite relationships. Overall, beyond the substantial influence of building characteristics and demographic features, the composition and configuration of land use are also significantly related to REPC. These findings demonstrate the role of neighborhood-scale urban morphology in shaping residential energy consumption and provide implications from the perspective of landscape planning in heating-dominated climates.

1. Introduction

Over the coming 30 years, the world's urban population is projected to rise by 2.5 billion (Mahtta et al., 2022), which is expected to accelerate urbanization and drive profound changes in land use and land cover (LULC). Urban expansion often involves the conversion of natural and agricultural lands into built-up areas, leading to the enlargement of impervious surfaces and restructuring of urban morphology (Frolking et al., 2024; Liu et al., 2020). Many studies have found that such transformations intensify the urban heat island (UHI) effect, as impervious surfaces absorb and retain heat, thereby elevating land surface temperature (LST) (Dev Roy et al., 2025; Kara and Yavuz, 2025). However, while the adverse public health impacts associated with intensified summer thermal conditions are well documented, the seasonal variability in the implications of UHI effects, especially the potential differentiated impacts on residential energy consumption in winter, requires further examination. Challenges such as limited data availability, inconsistent variable characterization, and differences in climate contexts and spatial scales continue to reinforce this knowledge gap (Li et al., 2023; Yu et al., 2020). Addressing seasonal dynamics is also important for developing more comprehensive and balanced urban climate adaptation strategies.

In the context of reducing building or residential energy consumption, different types of LULC have been shown to exert varying effects, underscoring the need for further investigation. In hot-summer regions, green space can contribute to residential energy savings by cooling surrounding areas and shielding buildings from solar radiation (Tsoka et al., 2021; Zhu et al., 2022a). However, a study in Harbin, a city in China with a severe cold climate, found that lower green space ratios may actually help reduce heating energy demand, particularly in urbanized areas (Leng et al., 2020). Similarly, a study conducted in Xi'an, located in the cold climatic region of China, found that the vegetation

* Corresponding author at: Institute of Environmental Sciences (CML), Leiden University, Einsteinweg 2, Leiden 2333 CC, The Netherlands.
E-mail address: h.yu@cml.leidenuniv.nl (H. Yu).

https://doi.org/10.1016/j.scs.2026.107449
Received 11 October 2025; Received in revised form 24 March 2026; Accepted 26 April 2026
Available online 30 April 2026

increased building heating load by 2.8% -7.16% depending on weather conditions (Ge et al., 2024). By contrast, a study in Eindhoven, a city in the Netherlands, reported a negative correlation between normalized difference vegetation index (NDVI), a remote sensing–based indicator of vegetation greenness and coverage, and energy demand (Chen et al., 2020). Beyond green spaces, blue infrastructure (nature and semi-natural water bodies) has also been identified as a factor in mitigating UHI effects and cooling urban environments (H. Chen et al., 2023; Zhou et al., 2024), thereby influencing building energy consumption, although its effectiveness depends on characteristics such as size, shape, and surrounding land use (Jandaghian and Colombo, 2024). Meanwhile, buildings' geometric characteristics also show influence on building energy consumption. For example, energy analyses based on geometrical models of residential buildings in London showed that high-rise buildings with greater plan depths achieve higher energy efficiency (Ahmadian et al., 2021). A Pareto optimization study further demonstrated that an optimized building's shape can achieve multiple objectives, including saving energy consumption, increasing photovoltaic energy potential and sunlight hours, and indicated that high-rise buildings with large volumes and small shape factors (the ratio of building surface area to volume) have lower energy use intensity (Liu et al., 2023). Collectively, these findings indicate that land use types, e.g., green, blue, or grey (built) infrastructure, exert distinct and sometimes opposing impacts on building energy consumption, and that their effects may amplify or offset each other. Therefore, to fully capture the effects of different land use types, it is essential to adopt an integrative approach that considers multiple land use types simultaneously rather than in isolation.

Urban morphology offers such an integrative perspective. Broadly defined as the study of urban form and the processes that shape it over time (Oliveira, 2020), it encompasses physical dimensions such as shape, structure, and function (Javanroodi et al., 2023) as well as the agents driving these changes. Urban morphology indicators (UMIs) provide a quantitative framework to integrate different LULC types with related socio-economic variables. Early classifications include the Local Climate Zone (LCZ) system (Stewart and Oke, 2012), while more recent approaches, such as the Green Infrastructure Typology (GIT) (Bartesaghi-Koc et al., 2020), mainly focus on the spatial interactions of natural and built elements, generally excluding socio-economic driving factors. However, studies from the urban metabolism perspective have identified facilitators/constraints, needs, and drivers as three key components (Dijst et al., 2018) influencing the spatial and temporal patterns of urban energy and water consumption (Voskamp et al., 2020), encompassing spatial, infrastructure and consumer-related characteristics (Voskamp et al., 2021). Meanwhile, recent studies have increasingly employed landscape metrics (LMs) to characterize spatial and infrastructural patterns from the perspectives of composition and configuration (Costanza et al., 2019; Hou and Estoque, 2020; Li et al., 2023; Lin et al., 2025; Yang et al., 2024).

Most existing studies have analyzed UMIs at the city scale (Chen et al., 2020; Zheng et al., 2018), with some extending to national-scale analyses (Labetski et al., 2023), or narrowing down to neighborhoods (Allen-Dumas et al., 2020). While large-scale studies provide a broad overview of morphological characteristics, the neighborhood scale offers practical advantages for applications (Lyu et al., 2024). Regarding the methodology, prior research can be broadly categorized into simulation-based and data-driven approaches. Simulation-based methods, often involving environmental or energy modeling (Liu et al., 2023; Zhu et al., 2022a), are valuable for exploring mechanisms but tend to be time-intensive and constrained by assumptions that limit applicability. In contrast, data-driven approaches rely on empirical data, producing results more closely aligned with real-world urban contexts and therefore more relevant for planning and policy (Zhou et al., 2023). Building on these advantages and leveraging extensive open datasets in the Netherlands, this study adopts a data-driven approach to examine the impacts of UMIs on residential energy consumption per capita (REPC) at the neighborhood scale. To sufficiently capture the spatial interactions across neighborhoods, a Spatial Durbin Model (SDM) is employed. Widely used in spatial econometrics, the SDM has been applied to issues where spatial dependence and spillover effects are critical, such as regional economic growth (Atikah et al., 2021), environmental pollution (Zhao and Wang, 2022), and urban vitality (Jiang and Huang, 2024). Unlike traditional regression models, the SDM explicitly accounts for spillover effects, i.e., the influence of one area on outcomes in neighboring areas, which makes it particularly suitable for neighborhood-scale studies where spatial autocorrelation is often present.

The residential sector in the Netherlands accounted for 16.8% of the country's total final energy consumption in 2022 ("The Netherlands - Countries & Regions," n.d.). About 73.3% of residential energy use is for heating in the Netherlands for the year of 2021, with gas dominating the Dutch heating sector (European Commission. Joint Research Centre, 2024). Most government measures to reduce residential energy consumption have focused on single buildings, such as housing refurbishment, energy labeling, and the promotion of renewable energy sources, which have proven effective in lowering household energy demand. However, broader-scale strategies that consider interactions between green, blue, and grey land uses remain underexplored and should be more systematically integrated into energy reduction efforts (Yang et al., 2025; Zhou et al., 2025). This study makes three contributions. First, it develops and applies a systematic framework to define and classify UMIs at the neighborhood scale in the Dutch context. Second, it directly examines the relationships between UMIs and residential energy consumption per capita using neighborhood-level data. Third, it employs an SDM to capture spatial dependence and spillover effects, demonstrating the potential of spatial econometric methods for urban spatial research.

2. Methodology

2.1. Study area and climate conditions

Situated along the North Sea, the Netherlands is classified as having a temperate oceanic climate (Köppen climate type Cfb), characterized by mild summers and relatively evenly distributed precipitation throughout the year (Beck et al., 2023). According to ASHRAE climate zoning, the Netherlands falls within Climate Zone 4, which is associated with moderate heating demand ("Weather Data Center," n.d.). The annual heating degree days (HDD) for the Netherlands were estimated to range from approximately 2200 to 2400 °C·days in recent years ("Cooling and heating degree days by country - monthly data," n.d.). Climate details and contextual comparisons are provided in Supplementary Material S1.

Neighborhoods were selected as the spatial unit of analysis due to the availability of residential energy data and the feasibility of computing all independent variables at the same scale. According to CBS (Statistiek, 2025a), based on registered address density, a total of 14,317 neighborhoods are classified into five levels of urbanity (1-5, from urban to rural). The distribution of these five urbanity levels is shown in S2.

2.2. Research design

The research methodology comprised several steps, including I) data collection and preparation, II) variable identification and model specification, as well as III) results interpretation and discussion, as summarized in Fig. 1.

2.3. Data collection and preparation

2.3.1. Data collection

Land use and vegetation maps were derived originally from the National Land Use Database of the Netherlands (LGN) and National Institute for Public Health and the Environment (RIVM). Demographic

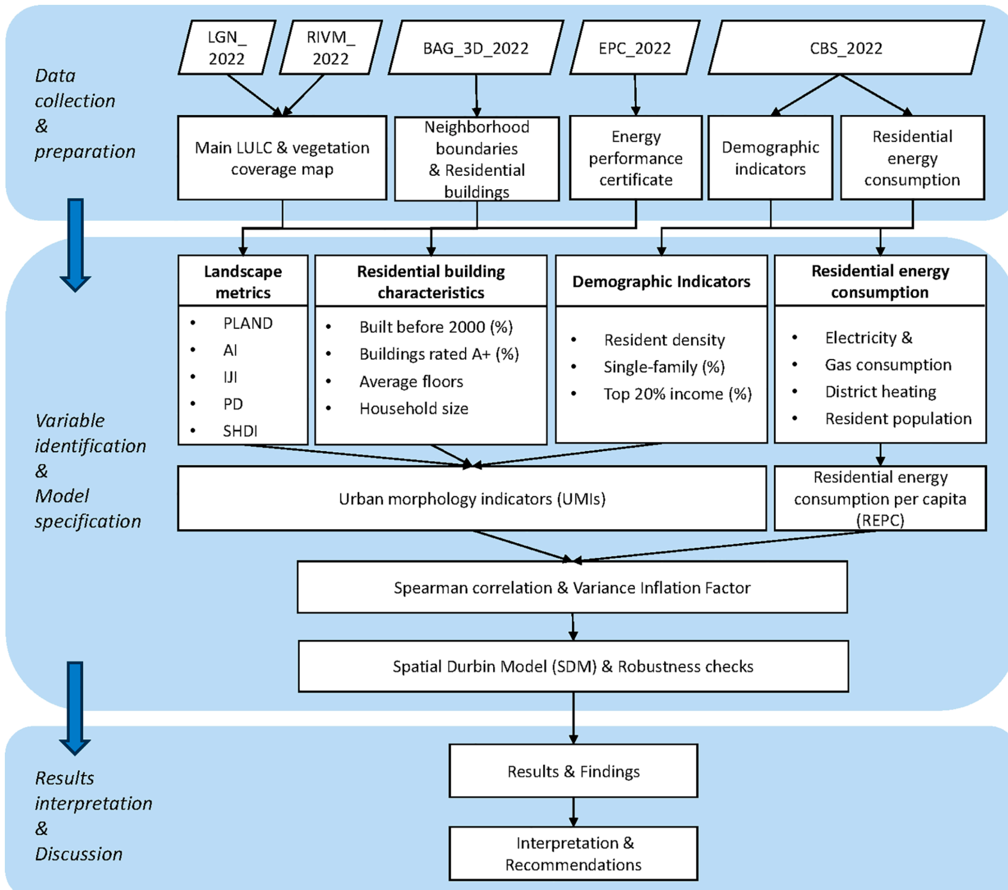

Fig. 1. Research framework (Abbreviations are defined in Section 2.4).

indicators were primarily obtained from the neighborhood's key figures provided by Statistics Netherlands (CBS). Building characteristics variables were compiled from both the Basic Registration of Addresses and Buildings (BAG) and CBS, supplemented with information of the Energy Performance Certificates (EPC) from Netherlands Enterprise Agency (RVO). The references for the dataset above are listed in Table 1. The dependent variable, residential energy consumption per capita (REPC), was constructed at the neighborhood level by aggregating average annual electricity, gas, and district heating consumption and dividing by the resident population.

This study uses data from 2022, the most recent year available when the analysis was conducted. It should be noted that although 2022 was affected by the European energy price crisis and overall household energy consumption declined, this decline occurred in a broadly uniform manner across the country (Statistiek, 2025b). Given that this study focuses on cross-sectional variation among neighborhoods rather than absolute consumption levels, the estimated relationships are unlikely to be affected by the temporary conditions of 2022.

Table 1
Data sources used in this study (2022).

Data type	Purpose	Abbreviation and source
Main land use types	To reclassify the main land use and land cover	LGN, National land use database of the Netherlands ("LGN - Basiskaart," n.d.)
Vegetation coverage	To reclassify vegetation categories and their coverage	RIVM, The maps of trees, shrubs, and grass ("Maps | Natural Capital Atlas," n.d.; Overheidspublicaties, n.d., n.d.)
Building geometry	To select residential buildings and identify them within neighborhood boundaries	BAG, Data for 2022 was obtained previously. The most recent version of the data is publicly available ("3DBAG," n.d.)
Building energy label	To identify energy labels of residential buildings selected from the BAG	RVO, Data for 2022 was obtained directly from RVO. The most recent version of the data is publicly available ("National Georegister," n.d.)
Demographic data	To determine demographic indicators	CBS, Key figures for districts and neighborhoods, 2022 (Statistiek, 2025a)
Energy consumption	To calculate residential energy consumption per capita (REPC)	

2.3.2. Data preparation

a. Neighborhood residential energy consumption

Neighborhood-level total energy consumption was decomposed into electricity, natural gas, and district heating.

Total electricity or gas consumption at the neighborhood level were estimated as:

$$E_{ele/gas} = G_{ave\_neigh} * N_{neigh\_units} * P_{occupied} \tag{1}$$

Where G_{ave_neigh} is the average annual electricity or gas consumption across all housing unit types, calculated based on occupied housing units (See Supplementary Material S3.3), N_{neigh_units} is the total number of living units in each neighborhood, $P_{occupied}$ is the proportion of occupied living units within each neighborhood.

For district heating, it was estimated as:

$$E_{district} = G_{ave\_national} * N_{neigh\_units} * P_{district} \tag{2}$$

Where $G_{ave\_national}$ is the national average annual district heating consumption per living unit, and $P_{district}$ is the proportion of living units (both occupied and vacant) in a neighborhood connected to the district heating system (see Supplementary Material S3.3). Since $G_{ave\_national}$ is not directly available, it was derived from the 2024 district heating network sustainability report (2022 data) ("Rapporteer over de duurzaamheid van uw warmtenet," n.d.). Although the estimation of $G_{ave\_national}$ is necessarily coarse (see Supplementary Material S3.4), the relatively low share of living units connected to district heating, only 6-7% nationally (Netherlands, 2025), implies that regional differences are unlikely to be substantially affected.

All energy carriers were harmonized and converted into kWh prior to aggregation. Additional details and the overall calculation workflow are provided in Supplementary Material S3.

a. Land use and vegetation cover maps

To ensure consistency with the RIVM dataset of vegetation cover, the original LGN 2022 data, with nationwide coverage at a 5-meter spatial resolution and covering 51 land use types, were resampled to a 10-meter resolution and reclassified into five main land use categories: Agriculture, Built, Green, Water, and Others. The reclassification map is presented in Fig. 2.

Buildings and roads are jointly classified as built-up land due to their similar impervious characteristics and shared influence on the local microclimate, particularly in relation to urban heat island (UHI) effects. The Green category refers to vegetated land cover (e.g., areas dominated by trees, shrubs, and grass). The rules used for manual reclassification are provided in Supplementary Material S4.

We incorporated vegetation data from RIVM, which provides high-resolution (10 m) maps of tree, shrub, and grass cover at the grid-cell level (Fig. 3, left). After combining maps of grass cover, shrub cover, and tree cover in ArcGIS Pro (v. 3.1.2), the resulting vegetation cover map complements the reclassified LGN map by providing a more detailed representation of vegetation cover, in particular capturing tree canopy alongside shrubs and grass.

Building on the assumption that both vegetation height and coverage may influence neighborhood-scale microclimates (Xi et al., 2023), and that these microclimates in turn affect residential energy consumption (Ge et al., 2024; Zhu et al., 2023), we further categorized green spaces derived from the RIVM dataset (Fig. 3, right).

A two-dimensional quadrant framework based on vegetation height (Short vs. Tall) and coverage (Sparse vs. Dense) was applied, with grass

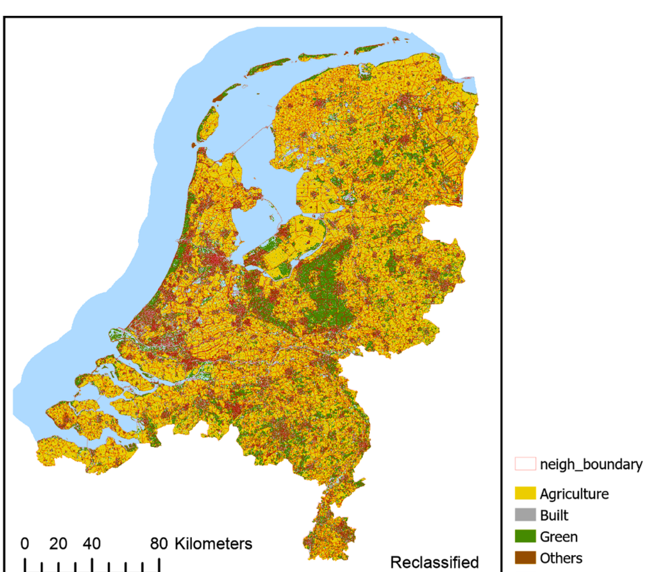

Fig. 2. Reclassified LGN land use map with neighborhood boundaries.

and shrubs defined as short vegetation and trees as tall vegetation. This resulted in four green space categories, of which Dense_Short (49.10%) and Dense_Tall (26.95%) together accounted for more than 75% of vegetated areas and were therefore selected as key variables for further statistical analysis. Sparse_Short and Sparse_Tall were retained in the vegetation classification map used for landscape metric calculation, and therefore influenced the values of Dense_Short and Dense_Tall.

2.4. *Variable identification*

We structured a broader categorization of Urban Morphology Indicators (UMIs) at neighborhoods level by including demographic indicators, residential building characteristics and landscape metrics (LMs).

2.4.1. *Demographic indicators*

Neighborhood-level demographic data were obtained from CBS (Statistiek, 2025a), covering aspects such as population density (pop_density), household size (hh_size) and characteristics (SF_pc), and income levels (inc_hi_pc). These indicators were selected to capture regional disparities as well as neighborhood-specific socioeconomic characteristics that may influence residential energy consumption. They were included to control for demographic differences and reduce the risk that the effects of landscape metrics are confounded with socioeconomic factors. All selected demographic indicators, including definitions and descriptive statistics, are summarized in Table 2.

2.4.2. *Residential buildings characteristics*

Residential buildings from BAG with a designated "main living function" were selected and spatially linked to neighborhoods by intersecting building geometries with neighborhood boundaries in ArcGIS Pro (v. 3.1.2). Buildings split at neighborhood edges due to minor spatial mismatches were represented by their largest portion. Energy label data were then matched to those buildings, resulting in 5,338,549 residential buildings after processing. The definitions, data sources, and descriptive statistics are presented in Table 3.

2.4.3. *Landscape metrics (LMs)*

LMs are typically categorized into three hierarchical levels: patch-level, class-level, and landscape-level metrics, ranging from small to large spatial scales (Cai et al., 2023; Wu et al., 2025). In this study, we selected representative indicators from the class and landscape levels.

At the class-level, we included: Percentage of Landscape Class (PLAND), which measures the proportion of each land use type; Aggregation Index (AI), which quantifies the spatial cohesion or compactness of a certain land use type itself; and Interspersion and Juxtaposition Index (IJI), which evaluates the degree to which a given land use type is intermixed with others. The differences between AI and IJI are that AI focuses on the internal aggregation of a single land use type, while IJI considers the degree of intermixing with the other land use types, which is also influenced by the number of land use types. In many cases, while the PLAND values across neighborhoods are relatively similar, AI and IJI vary substantially, underscoring the necessity of jointly considering both composition and configuration (see Supplementary Material S6). At the landscape-level, we used: Patch Density (PD), to assess fragmentation by measuring the number of patches for all land use types, and Shannon's Diversity Index (SHDI), which quantifies the compositional diversity of the entire neighborhood.

All landscape metrics were calculated using Fragstats v4.2 (https://www.fragstats.org), based on two maps originally sourced from LGN and RIVM, and spatially divided according to neighborhood boundaries obtained from BAG. The calculation methods and descriptions of the selected landscape metrics are presented in Table 4.

Spearman correlation analysis was employed to identify highly correlated variables, as it is less sensitive to outliers and does not require normality assumptions (Wu et al., 2025) compared with Pearson

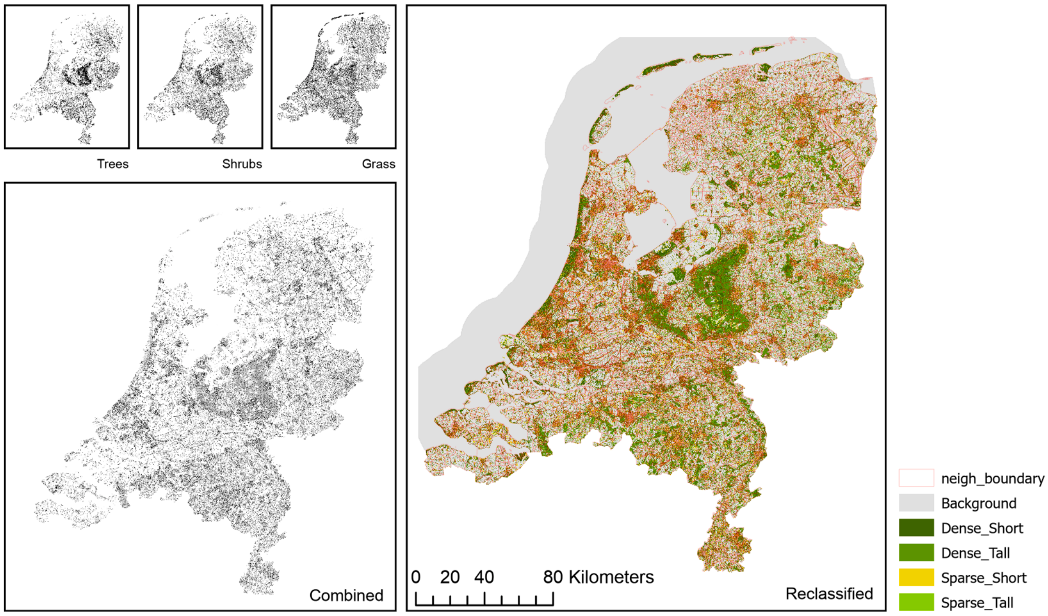

Fig. 3. Results of the combined RIVM maps and the vegetation classification.

Table 2
Neighborhood-level demographic indicators adopted in this study (n=10,580 neighborhoods included in the final analysis; corresponding abbreviations in the CBS documentation are provided in Supplementary Material S5.1).

UMIs (Demographic indicators)	Description	Mean	Median
pop_density	The number of residents divided by the land area in square kilometers [/km^2]	3493	2526
hh_size	Average persons per household	2.29	2.30
SF_pc	The percentage of single-family housing. Notably, CBS defines a single-family housing as any living unit with an individual entrance [%]	76.54	87.00
inc_hi_pc	Share of individuals in private households belonging to the national top 20% income group [%]	21.06	20.20

Table 3
Neighborhood-level residential building characteristics indicators adopted in this study (n=10,580 neighborhoods included in the final analysis; corresponding abbreviations in the CBS documentation are provided in Supplementary Material S5.1).

UMIs (Building characteristics)	Data source	Description	Mean	Median
pre2000_pc	CBS	The proportion of housing units constructed before 2000 [%]	80.70	89.00
Aplus_pc	BAG, RVO	Proportion of buildings with high energy efficiency labels, defined as labels A and above [%]	13.47	7.76
ave_floor	BAG	Average number of stories of residential buildings within a neighborhood, assuming a standard floor height of 3m. Derived as the neighborhood floor area ratio (FAR) divided by building density.	2.57	2.33

correlation analysis. Variance Inflation Factors (VIF) were then calculated, and variables with VIFs exceeding 5 were excluded. The variable

Table 4
Class- and landscape-level LMs (as part of UMIs) adopted in this study.

UMIs (Class-level metrics)	Formula	Description
PLAND (Percentage of Landscape Class)	$PLANDi = \frac{\sum_{j=1}^{n} a_{ij}}{A} \cdot 100$	Proportion of the total landscape occupied by land use type *i*
AI (Aggregation Index)	$AIi = \left(\frac{g_{ii}}{g_{ii}^{max}}\right) \cdot 100$	Degree of aggregation of land use type *i*, based on the proportion of like adjacency pairs
IJI (Interspersion and Juxtaposition Index)	$IJIi = \frac{-\sum_{k=1, k\neq i}^{m} \left(\frac{g_{ik}}{\sum_{k\neq i} g_{ik}} \ln\left(\frac{g_{ik}}{\sum_{k\neq i} g_{ik}}\right)\right)}{\ln(m-1)} \cdot 100$	Degree of evenness in the distribution of edge adjacencies between land use type *i* and other types *k*
UMIs (Landscape-level metrics)	**Formula**	**Description**
PD (Patch Density)	$PD = \frac{\sum_{i=1}^{m} n_i}{A} \cdot 10^6$	Total number of patches per km^2 of landscape area
SHDI (Shannon's Diversity Index)	$SHDI = -\sum_{i=1}^{m} (Pi * lnPi)$	Landscape diversity considering both land use richness and proportional distribution

Notes : a_{ij} : *Area of patch j of class i*,
A : *Total landscape area*,
n_i : *Number of patches of class i*,
g_{ik} : *Number of adjancencies between class i and class k*,
g_{ii}^{max} : *Maximum possible like adjancies for class i*,
m : *Number of land use types*,
Pi : *Proportion of the landscape occupied by land use type i*.

selection procedure is detailed in Supplementary Material S5.2.

The initial dataset consisted of 14,317 neighborhoods. Prior to merging with the landscape metrics derived from Fragstats, 11,418 neighborhoods were successfully matched across the CBS and BAG datasets. After excluding neighborhoods with missing values (NaN) in the selected landscape metrics, the final analytical sample comprises 10,580 neighborhoods, representing approximately 92.27% of the

Dutch population. Within the final sample, more than 69% of neighborhoods have a land area smaller than 2.5 km^2, and over 80% have fewer than 3,000 residents. Details of the data filtering process are provided in Supplementary Material S7.

2.5. Model specification

Spatial econometric models (LeSage & Pace, 2009) are adopted in this neighborhood-level study, as they are specifically designed to capture spatial dependence and spillover effects among neighborhoods (Zhang et al., 2023). In summary, there are several reasons for adopting spatial econometric models to examine the relationship between UMIs and REPC:

1. Significant spatial autocorrelation in REPC values was identified through the Global Moran's I test (see Supplementary Material S9), indicating clustered residential energy consumption patterns. However, this test does not reveal whether the explanatory variables exhibit spatial autocorrelation, thus requiring further diagnostic analyses for model specification.
2. To capture spillover effects from green spaces. Green infrastructure in one neighborhood may influence microclimates in adjacent areas and in turn affect residential energy consumption in neighboring neighborhoods, particularly near shared boundaries.
3. Uncertainties in neighborhood boundary delineation may introduce arbitrariness. Spatial econometric methods help mitigate boundary effects by explicitly incorporating interactions among adjacent areas.

Table 5 provides an overview of the key differences among commonly used spatial econometric models. As shown in S11, all spatial models outperform OLS based on Lagrange Multiplier (LM) tests, and the Spatial Durbin Model (SDM) provides the best fit according to Likelihood Ratio (LR) tests. Therefore, the SDM is adopted for subsequent analyses.

The spatial weight matrix is constructed using a k-nearest neighbors specification with $k = 6$, reflecting the median number of adjacent neighborhoods in the complete neighborhood map (see S8). This choice also ensures a consistent spatial structure in the presence of potential fragmentation and isolated units after sample filtering.

Importantly, the statistical coefficients from the SDM cannot be directly interpreted as marginal effects due to spatial feedback effects (LeSage & Pace, 2009), as changes in one neighborhood may spill over to neighboring areas and feed back through the spatial network. Impact measures are therefore computed using the spatial multiplier to translate the estimated coefficients into interpretable direct and indirect impacts (Elhorst, 2014; Zhang et al., 2023). As illustrated in Supplementary Material S10, the direct impacts represent the average marginal effect of local characteristics on a neighborhood's own REPC, whereas the indirect impacts capture average spillover effects on neighboring neighborhoods transmitted through the spatial weights matrix W (LeSage & Pace, 2009).

Table 5
The comparison between commonly used spatial econometric models and Ordinary Least Squares (OLS).

Model	Spatial Term(s)	Main Purpose	Equation Form
SAR (Spatial Autoregressive Model)	**WY**	Captures spatial dependence in outcomes	$Y = \rho WY + X\beta + \varepsilon$
SEM (Spatial Error Model)	**W**ε	Controls for spatially autocorrelated errors	$Y = X\beta + \mu$, *with* $\mu = \lambda W\mu + \varepsilon$
SDM (Spatial Durbin Model)	**WY, WX**	Captures spatial dependence and spatial spillovers	$Y = \rho WY + X\beta + WX\theta + \varepsilon$
OLS (Ordinary Least Squares)	/	Serves as a baseline, assumes independence across units.	$Y = X\beta + \varepsilon$

Notes: β : Coefficients for X (effects of focal X values); ρ: Spatial autoregressive coefficient (effects of neighboring Y values); ε: Error term; μ: Spatially correlated error term; λ: Spatial error coefficient (effects of spatially correlated errors); θ : Coefficients for spatially lagged independent variables (effects of neighboring X values).

3. Results

3.1. Residential energy consumption in Dutch neighborhoods

The data show substantial variation in both residential energy consumption (REC) and residential energy consumption per capita (REPC) across neighborhoods with different levels of urbanity. As illustrated in Fig. 4, total REC generally declines from the most urban to the most rural areas, whereas REPC exhibits a slight upward trend. In the most urbanized neighborhoods, the median total REC is around 9.94 GWh, with a median REPC of approximately 5.42 MWh. By contrast, the most rural neighborhoods consume about 2.70 GWh in total, roughly one-fourth of the most urbanized ones, but display higher REPC, around 6.9 MWh, reflecting lower population densities (see S6).

REPC is used as the dependent variable to ensure meaningful comparisons across neighborhoods, as normalizing energy use at the individual level reduces sensitivity to differences in neighborhood size, household numbers, and other neighborhood-level structural differences.

As shown in the Moran scatterplot (Fig. 5, left), the dependent variable REPC exhibits positive spatial autocorrelation, indicating that neighborhoods with high (or low) values tend to be surrounded by others with similarly high (or low) values.

When compared with the spatial distribution of urbanity levels (see Supplementary Material S2), Fig. 5 (right) shows that higher REPC values are clustered in eastern and northern rural areas, whereas lower values are concentrated in the more urbanized western region, suggesting a potential urban-rural contrast.

3.2. Spatial Durbin model of selected variables

3.2.1. Grouped variable impacts

We used block-wise model comparisons to evaluate the relative joint contribution of each variable group (Fig. 6). Starting from the full model that includes all groups, we remove one group at a time and then compare the resulting Akaike Information Criterion (AIC) and Bayesian Information Criterion (BIC) values to those of the full model. By construction, larger ΔAIC/ΔBIC values indicate the model fit worsens when that group is removed, which means that the group has greater explanatory importance. The numerical summary of model comparisons is provided in Supplementary Material S12.

In terms of explanatory importance, building-characteristics variables dominate, followed by those of demographic indicators and then landscape metrics. Removing building-characteristics variables produces the largest increases in AIC and BIC ($\Delta IC > 2600$), clearly identifying this block as the most influential. Excluding demographic indicators results in intermediate increases ($\Delta IC > 1300$), reflecting substantial but secondary importance. Although landscape metrics show the smallest increases ($300 < \Delta IC < 600$), these values still far exceed the conventional cutoff ($\Delta IC \geq 10$), confirming that their contribution is meaningful.

3.2.2. Individual-variable impacts

Impact measures are required to represent the effects of each explanatory variable on the focal unit and its neighbors (see Section 2.5). All explanatory variables were standardized using z-scores to ensure comparability across variables with different units, while the

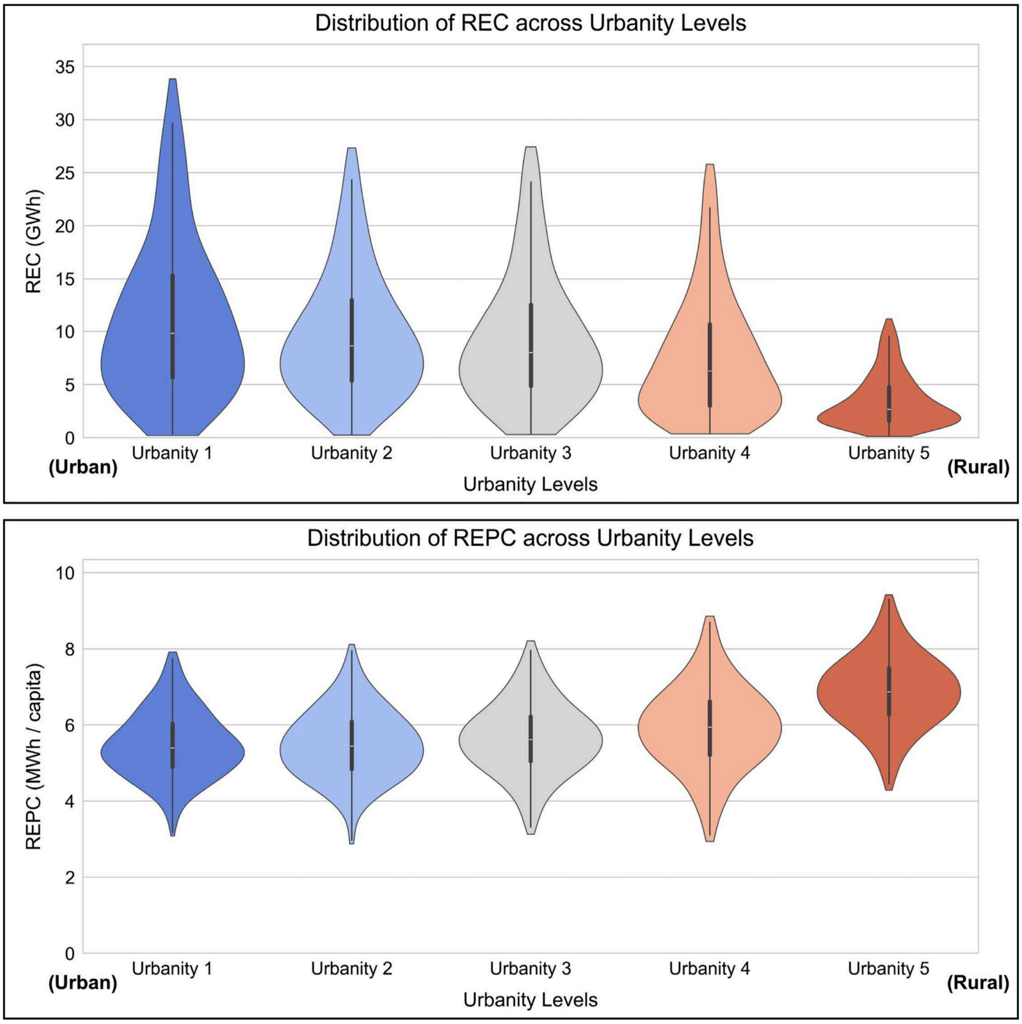

Fig. 4. REC and REPC across neighborhood urbanity levels (n=10,580, REC is reported in GWh, while REPC is expressed in MWh per capita for clarity).

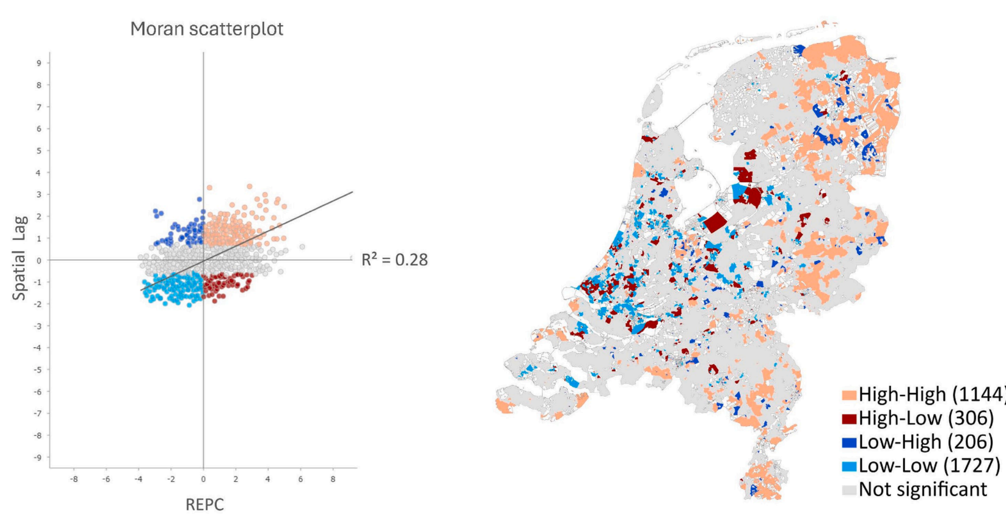

Fig. 5. The Moran scatterplot of REPC and the spatial distribution of its autocorrelation.

dependent variable (REPC) was log-transformed to facilitate interpretation of estimated impacts. The estimated impacts as well as model statistics were calculated in **R** and reported in Table 6.

a. Demographic and building characteristics

Figure 7 presents the direct, indirect, and total impacts of demographic indicators and building characteristics. Among demographic

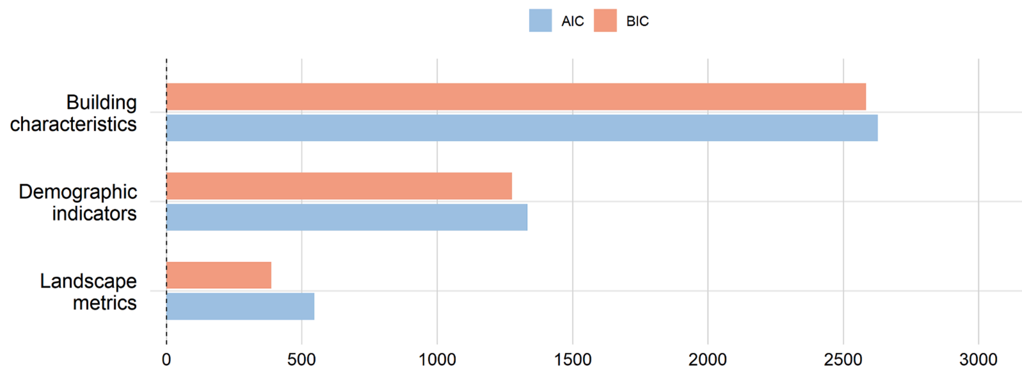

Fig. 6. Block-wise model comparison of ΔAIC and ΔBIC.

Table 6
Estimated results of the Spatial Durbin Model (SDM, n = 10,580, KNN = 6) for residential energy consumption per capita (REPC).

Variables			SDM		
			Direct impacts	Indirect impacts	Total impacts
Demographic indicators		pop_density	-0.045***	-0.022***	-0.067***
		SF_pc	-0.003	0.051***	0.048***
		inc_hi_pc	0.078***	-0.032***	0.046***
		hh_size	-0.048***	-0.032***	-0.080***
Building characteristics		pre2000_pc	0.074***	-0.021**	0.053***
		ave_floor	0.017***	0.015*	0.032***
		Aplus_pc	-0.039***	0.021**	-0.018*
LMs	Water	PLAND	-0.002	-0.033***	-0.035***
		AI	0.005*	0	0.005
		IJI	-0.006***	-0.009	-0.015**
	Built	AI	-0.006**	-0.032***	-0.038***
		IJI	0.031***	0.007	0.038***
	Dense_Short	PLAND	-0.010***	-0.066***	-0.076***
		AI	0.004	0.045***	0.049***
	Dense_Tall	PLAND	0.009***	0.017*	0.026***
		AI	-0.008***	0.006	-0.002
	Landscape-level metrics	PD	0.017***	0.001	0.018***
		SHDI	-0.024***	0.002	-0.022***
Model Statistics					
R^2		0.515			
Log Likelihood		4098.63			
AIC		-8119			
BIC		-7836			

Note:.
* p-value <0.1,
** p-value <0.05,
*** p-value <0.01; LMs is referring to Landscape Metrics.; Impacts are rounded to three decimal places.

indicators, resident density (pop_density) and household size (hh_size) are the only two variables that show consistently negative direct and indirect impacts, resulting in strongly negative total impacts. Specifically, a one standard deviation increase in population density is associated with a 4.5% lower local REPC and an additional 2.2% lower REPC in surrounding neighborhoods, corresponding to an overall difference of approximately 6.7%. Household size shows a similar pattern, with comparable negative direct impacts (-0.048, p<0.01) and stronger negative indirect impacts (-0.032, p<0.01), yielding a substantial negative total impact (-0.080, p<0.01).

The share of single-family housing (SF_pc) has no significant direct impact on local REPC but is positively associated with REPC in surrounding areas (0.051, p<0.01), resulting in a significant positive total impact (0.048, p<0.01). Additionally, the proportion of high-income residents (inc_hi_pc) exhibits the strongest positive direct impact on REPC in the focal neighborhood (0.078, p<0.01), while showing a negative indirect impact on REPC in surrounding neighborhoods (-0.032, p<0.01), resulting in a net positive total impact (0.046, p<0.01).

Regarding building characteristics, both the share of buildings constructed before 2000 (pre2000_pc) and average number of floors (ave_floor) are positively associated with REPC in terms of total impacts (0.053, p<0.01 and 0.032, p<0.01). These impacts correspond to positive direct impacts of 7.4% for pre2000_pc and 1.7% for ave_floor. However, their indirect impacts differ in directions: ave_floor shows a positive indirect impact (0.015, p<0.1), whereas pre2000_pc is associated with a negative indirect impact (-0.021, p<0.05) on surrounding neighborhoods. Energy label rated above A (Aplus_pc) is negatively associated with local REPC (-0.039, p<0.01), but positively associated with REPC in surrounding neighborhoods (0.021, p<0.05), resulting in a modest negative total impact (-0.018, p<0.1).

b. Landscape Metrics

Figure 8 presents the direct, indirect, and total impacts of class-level and landscape-level Landscape Metrics (LMs). Variables are ordered and interpreted by land use type. Indicators of green spaces are derived from RIVM vegetation data, while built-up and water areas are based on reclassified LGN maps (see Section 2.3.2 b).

(I) For water areas:

The percentage of water area (PLAND_water) exerts a negative impact on REPC in surrounding neighborhoods (-0.033, p<0.01). Regarding spatial configuration, a higher aggregation index of water (AI_water) is associated with slightly higher local REPC. By contrast, a higher interspersion and juxtaposition index of water (IJI_water) is negatively associated with REPC through direct impacts (-0.006, p<0.01), resulting in an overall difference of 1.5% lower REPC.

(II) For built-up areas:

As a measure of spatial composition, PLAND_built was excluded due to its high correlation with resident density (pop_density) (see Supplementary Material S5.2). Regarding the spatial configuration, a higher interspersion and juxtaposition index of built areas (IJI_built) is associated with higher local REPC. Specifically, a one-unit increase in IJI_built corresponds to a 3.1% increase in local REPC. Consistent with this pattern, a higher aggregation index of built areas (AI_built) is negatively associated with both local and neighboring REPC (-0.006, p<0.05 and -0.032, p<0.01), resulting in a negative total impact (-0.038, p<0.01).

(III) For green areas:

PLAND_Dense_Short, representing the share of short vegetation such as grasslands and shrubs, is negatively associated with REPC through

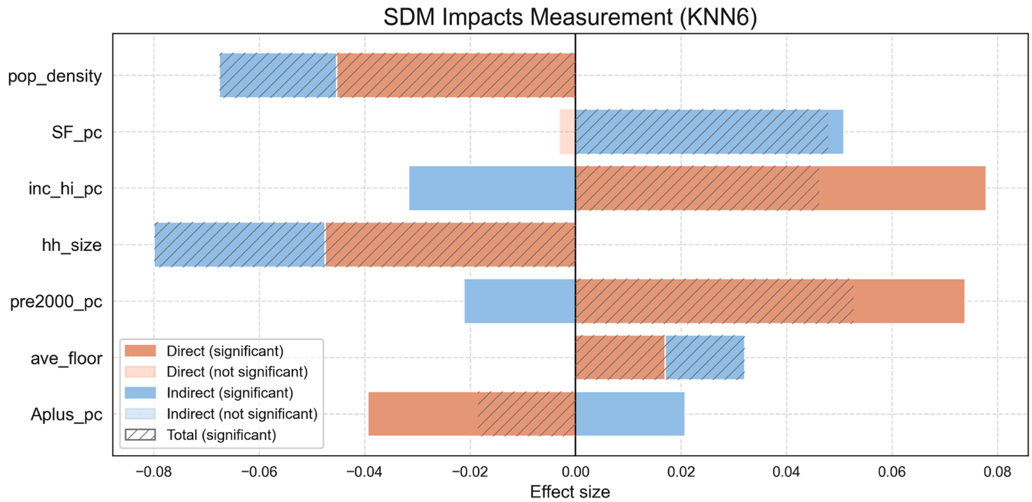

Fig. 7. Direct, indirect, and total impacts of demographic and building characteristics variables on REPC.

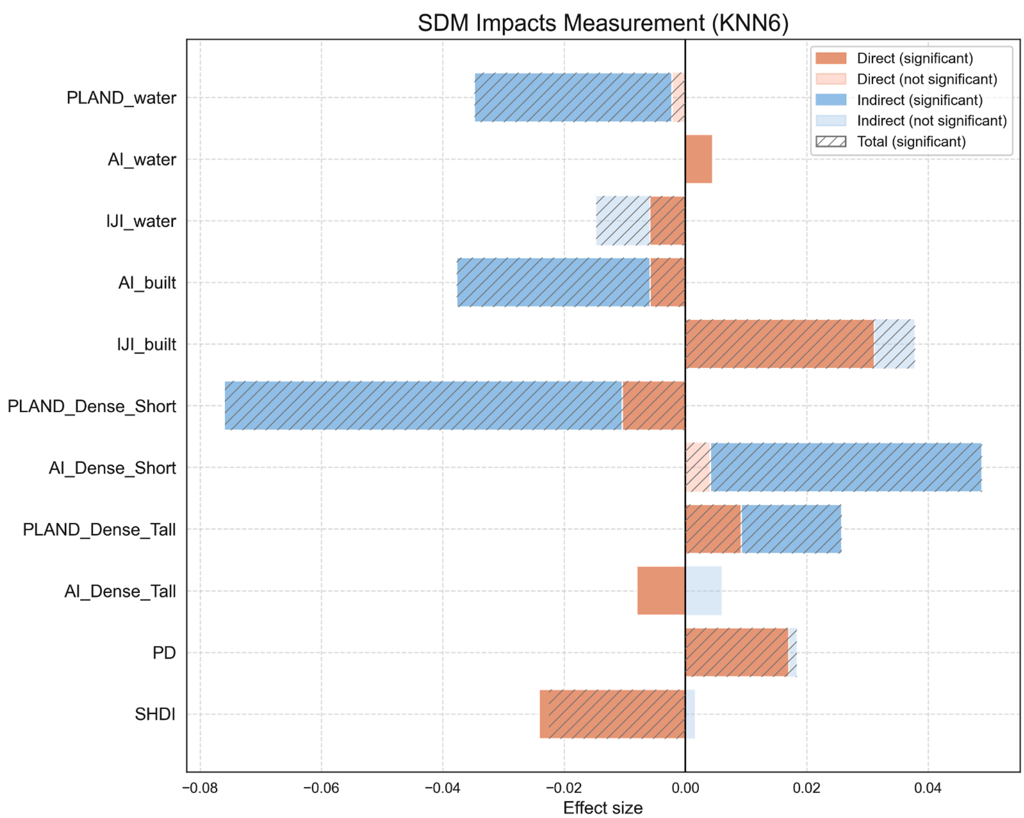

Fig. 8. Direct, indirect, and total impacts of landscape metrics on REPC.

both direct (-0.010, $p<0.01$) and indirect (-0.066, $p<0.01$) impacts, resulting in a significant negative total impact (-0.076, $p<0.01$). Regarding spatial configuration, a higher aggregation index of dense short vegetation (AI_Dense_Short) is associated with higher REPC in surrounding neighborhoods (0.045, $p<0.01$). In contrast, for tall vegetation, a higher proportion of tree cover is positively associated with REPC through both direct (0.009, $p<0.01$) and indirect (0.017, $p<0.1$) impacts, opposite in direction to that of short vegetation. With respect to configuration, higher aggregation index of tall vegetation (AI_Dense_Tall) is associated with lower local REPC (-0.008, $p<0.01$).

(IV) For landscape-level LMs:

At the landscape level, higher patch density (PD) is positively associated with local REPC (0.017, $p<0.01$). In contrast, a higher Shannon diversity index (SHDI) is negatively associated with local REPC (-0.024, $p<0.01$). These landscape-level metrics capture the overall heterogeneity of land use patterns.

3.2.3. *Robustness checks*

To test the robustness of the model, we experimented with multiple specifications of the spatial weights matrices. Besides the main specification (KNN=6), we also tested alternative matrices, including QUEEN contiguity, KNN=4, and KNN=8, while keeping the sample, transformations, and the estimation method fixed. The comparison of the results can be seen in Supplementary Material S13.

Consistency is defined as no change in significance status across matrices. Moreover, when effects are significant across all specifications, the sign must also remain consistent (significance levels may differ), whereas for uniformly non-significant effects, the sign is irrelevant. Across the alternative spatial-weight matrices, total impacts are fully stable (100% consistent), direct impacts show a high degree of robustness (≈94.4%), while indirect impacts are relatively more sensitive to matrix choice (≈72.2%). Overall, the main qualitative conclusions remain robust to alternative spatial-weight specifications.

4. Discussion

4.1. Broader structure of urban morphology indicators (UMIs) and corresponding policy implications

In this study, urban morphology is conceptualized broadly at the neighborhood scale, incorporating both physical landscape patterns and its underlying social and economic drivers. The block-wise model comparison (Fig. 6) reveals a clear hierarchy among the three groups of UMIs, with building characteristics showing the strongest influence, followed by demographic indicators and landscape metrics.

Firstly, the results suggest that the identified relationships between urban morphology and REPC are not limited to a specific type of neighborhood, but appear consistently across the study area. Secondly, improving building energy performance remains a fundamental strategy for reducing REPC. Measures such as neighborhood-scale renewal strategies, targeted retrofit programs, and subsidy schemes aimed at upgrading insulation, heating systems, and overall energy efficiency, particularly for high-rise and pre-2000 residential buildings, are therefore essential across all neighborhoods.

However, although landscape metrics contribute less than demographic and building characteristics variables, they still exert measurable effects on REPC and may provide additional opportunities for intervention through spatial planning. Although we did not further cluster the neighborhoods into specific types, given the existing differences between urbanized and rural neighborhoods, the priorities and significance of spatial planning strategies may vary in terms of feasibility and effectiveness.

To be specific, in highly urbanized neighborhoods, where land availability is limited and building density is high, spatial interventions may be more constrained. Nevertheless, the limited space also makes the efficient configuration of built-up areas and green infrastructure particularly important. For example, more aggregated buildings, more scattered water areas, and more aggregated tree-covered areas are associated with lower REPC. In lower-density neighborhoods, greater flexibility in both land-use composition and configuration allows spatial planning strategies to be implemented more easily. In addition to the favorable configurations identified in urbanized neighborhoods, a high proportion of grass-covered green spaces may be beneficial. The specific interpretations of spatial planning implications are further discussed in Section 4.2.

4.2. Influential LMs and neighborhood-scale spatial planning implications

Our findings highlight differentiated associations across water, built, and green areas in relation to REPC at the neighborhood scale. It is noteworthy that some variables showed significant indirect impacts without corresponding significant direct impacts (specifically, PLAND_water and AI_Dense_Short). Such patterns should be interpreted cautiously. In the SDM framework, indirect impacts represent average spillover effects transmitted through the spatial weights matrix W (LeSage & Pace, 2009). Therefore, they may capture spurious spatial associations arising from omitted variables or unobserved factors in the broader spatial context rather than purely local physical mechanisms.

First, the results showed that a greater extent of water bodies tends to reduce residential energy consumption per capita (REPC) in surrounding neighborhoods (PLAND_water), with significance observed only for the indirect impact. In addition, they appear to be more effective in lowering local REPC when they are spatially scattered and intermixed with other land uses (AI_water), although their direct impacts through AI and IJI remain relatively small. From a spatial planning perspective, these results imply that diversifying the spatial distribution of water areas can be more beneficial than concentrating water surfaces in large, continuous forms. For example, subdividing water surfaces with vegetated buffers to create smaller and more evenly distributed patches may better support energy-efficient neighborhood environments in the Netherlands.

Second, built-up areas are more effective for reducing local REPC when they are more compact, avoiding excessive intermixing with other land uses, as reflected by higher aggregation (AI_built) and lower interspersion (IJI_built). Such spatial configurations may help retain ambient heat around buildings and reduce heat loss. The results further indicate a spillover effect, whereby more aggregated built-up forms (AI_built) are also associated with lower REPC in neighboring areas. Overall, more compact buildings and associated transportation infrastructure are associated with reduced REPC at both local and neighboring scales.

Third, among various green space categories, dense short vegetation (e.g., grasslands) and dense tall vegetation (e.g., forests) are selected as the primary focus. In terms of composition, both direct and indirect impacts are observed for these two types, but in opposite directions. A higher proportion of grasslands is associated with lower residential energy use, whereas a higher proportion of forests corresponds to higher energy use, with indirect impacts dominating in both cases. From a configurational perspective, aggregated grasslands tend to increase neighboring REPC through indirect pathways, while aggregated forests reduce local REPC via direct impacts. Even though the indirect impacts of aggregated grasslands need to be interpreted with caution, these contrasting patterns underline the importance of distinguishing vegetation types when optimizing spatial composition and configuration of green areas for residential energy conservation.

Fourth, the results of overall landscape-level metrics, PD and SHDI, suggest that, in general, landscapes characterized by lower patch density and higher land use diversity tend to have lower REPC. However, as shown above, different land use types exhibit distinct patterns in how their spatial composition and configuration relate to REPC.

4.3. Linking urban morphology to residential energy consumption: insights from land surface temperature (LST)

Most previous studies emphasize the role of urban green, blue, and grey infrastructure in mitigating land surface temperature (LST) (Dev Roy et al., 2025; Guo et al., 2019; Wang et al., 2024; Wu et al., 2025; Yang et al., 2020) and urban heating islands (UHIs) broadly (Hou and Estoque, 2020; Yang et al., 2024), with a predominant focus on summer periods.

Water bodies are generally found to exert stronger cooling than insulation effects (Cureau et al., 2023; Yang et al., 2020), with larger water surfaces associated with greater LST reductions (Zhou et al., 2022), even in relatively cold climates such as Copenhagen (Yang et al., 2020). For built-up areas, existing evidence shows mixed LST responses to building form: taller buildings may reduce summer LST through shading and ventilation (Wang et al., 2025), whereas higher density and coverage tend to increase it (Han, 2023). Vegetation effects differ by type, for example, forests typically provide stronger cooling than grasslands in summer (Yu et al., 2020; Zhu et al., 2022b), while also exhibiting a slight warming effect during winter (Li et al., 2025). In terms of configuration, higher intermixing of impervious surface (higher IJI) has been reported to mitigate UHIs in hot climates (Yang et al., 2024). Consistent with this, studies indicate that stronger mixing of built and natural land can reduce LST and thereby cooling demand (Masoudi and Tan, 2019; Zhu et al., 2022b). Some studies further report the existence of nonlinear relationships between landscape metrics, building characteristics, and LST using machine learning methods (Y. Chen et al., 2023; Lin et al., 2025; Qi et al., 2025). Overall, our findings are complementary to previous evidence on how LST responds to urban morphology indicators (UMIs), yet the implications for energy demand may differ between cooling-and heating-dominated contexts.

Building on this literature, and considering the Dutch residential energy context in which approximately 73.3% of residential energy consumption is used for space heating (European Commission. Joint Research Centre, 2024), we hypothesized that UMIs associated with higher per-capita residential energy consumption (REPC) would be linked to lower local temperature, as reflected by lower LST. To further explore the connections between UMIs and REPC via LST, we conducted an additional exploratory analysis using the 2022 neighborhood-level median wintertime LST as a proxy for local microclimatic conditions.

Consistent with this expectation, a significant negative Spearman correlation was observed between REPC and winter median LST ($\rho = -0.405$). Moreover, for five (IJI_water, AI_built, IJI_built, PLAND_Dense_Short, PLAND_Dense_Tall) of the seven landscape metrics that exhibited significant direct impacts on REPC in SDM, the direction of their associations with LST was opposite to that with REPC, suggesting a potential role of LST in mediating the relationship between UMIs and REPC (details in Supplementary Material S14). While LST is a representative indicator of neighborhood-scale microclimate, other factors such as wind speed, air temperature, shading, and humidity also influence heating demand. As such, this analysis is intended as a supplementary and exploratory validation of the main SDM results.

4.4. Limitations

This study provides a national-scale assessment of neighborhood-level relationships between broader urban morphology indicators (UMIs) and residential energy consumption per capita (REPC) in the Netherlands, but several limitations should be acknowledged.

First, data availability constrained variable selection. Regarding building characteristics, the analysis was limited to residential buildings, excluding buildings with combined living functions. Regarding land use types, agricultural land was excluded to avoid excessive neighborhood loss, although agricultural grasslands may function similarly to urban short vegetation.

Second, neighborhoods were adopted as the spatial unit of analysis for practical reasons, but this choice introduces scale-related uncertainties. Although the use of the SDM helps account for spatial spillover effects and may partially mitigate these biases, the analysis remains subject to the modifiable areal unit problem (MAUP) inherent in administrative boundaries.

Third, neighborhood-level residential energy consumption data were available only on an annual scale. Although winter land surface temperature (LST) was used as an exploratory proxy, and space heating accounts for 73.3% of residential energy use in the Netherlands while energy use for cooling is minimal, seasonally resolved energy data would allow a more robust assessment of seasonal mechanisms.

Fourth, while the Spatial Durbin Model (SDM) was selected based on diagnostic tests, it remains a linear and globally homogeneous framework and cannot capture potential nonlinear or spatially varying relationships, even though demographic indicators were included to account for contextual differences.

Finally, the winter LST-based analyses and Spearman correlations are exploratory. Although they largely support our findings, the SDM results should still be regarded as providing suggestive evidence of associations rather than establishing the underlying causal mechanisms.

Future studies could further explore the mechanisms underlying these statistical associations by integrating additional microclimate indicators and adopting complementary analytical approaches, such as machine learning techniques to capture complex and potentially nonlinear relationships. This could also be complemented by engineering-based simulation approaches to explicitly model physical processes. In addition, investigating interactions between landscape metrics and socioeconomic factors, as well as developing detailed neighborhood clustering, could support more context-specific interpretations and more tailored policy recommendations.

5. Conclusion

This study examined the relationship between broader urban morphology indicators (UMIs) and residential energy consumption per capita (REPC) across Dutch neighborhoods using a Spatial Durbin Model (SDM). The key findings provide implications for neighborhood-scale urban renewal, climate adaptation, and energy-sensitive spatial planning, particularly in a heating-dominated climate (Köppen climate type Cfb).

- Beyond the significant influence of building characteristics and demographic features, the composition and configuration of land use also exert measurable impacts on REPC.
- Across Dutch neighborhoods, land use diversity is generally associated with lower residential energy consumption, although each land use type may require an optimal spatial arrangement to realize this benefit.
- Compact forms of building and transportation infrastructure are consistently linked to lower REPC.
- More spatially interspersed water bodies are associated with lower REPC, although their impacts remain small.
- The extent of tree-covered areas is associated with higher REPC, whereas grass- and shrub-covered areas are associated with lower values. In both cases, the indirect impacts play a dominant role.
- Aggregated tree-covered areas are associated with lower local REPC, whereas aggregated grass- and shrub-covered areas show no significant association with local REPC, but are linked to higher REPC in neighboring areas, which should be interpreted with caution.

CRediT authorship contribution statement

Han Yu: Writing – original draft, Visualization, Methodology, Investigation, Funding acquisition, Formal analysis, Data curation, Conceptualization. **Mingming Hu:** Writing – review & editing, Supervision, Conceptualization. **Arnold Tukker:** Writing – review & editing, Supervision. **Peter Berrill:** Writing – review & editing, Supervision, Methodology, Data curation, Conceptualization.

Declaration of competing interest

The authors declare no conflict of interest.

Acknowledgements

The authors thank Joeri Morpurgo for his assistance with vegetation classification and data interpretation, and Jianhua Zhang for his valuable suggestions on the application of spatial econometric models.

The author would like to thank the China Scholarship Council (CSC) for funding the research project (No. 202306260030). The authors also acknowledge the Multigreen project (No. 48219704) under NWO "Merian Fund Cooperation China-The Netherlands (CAS) Green Cities 2019".

The authors used generative artificial intelligence tools to assist with language editing, stylistic refinement, and coding support. All scientific content, analyses, and interpretations were conducted by the authors.

Supplementary materials

Supplementary material associated with this article can be found, in the online version, at doi:10.1016/j.scs.2026.107449.

Appendix A

Abbreviations	Descriptions
LULC	Land Use and Land Cover
UHI	Urban Heat Island
LST	Land Surface Temperature
LMs	Landscape Metrics
EPC	Energy Performance Certificate
BAG	Basic Registration of Addresses and Buildings
CBS	Statistics Netherlands
RVO	Netherlands Enterprise Agency
HDD	Heating Degree Days
LGN	National Land Use in the Netherlands
RIVM	National Institute for Public Health and the Environment
REC	Residential Energy Consumption
REPC	Residential Energy Consumption per capita
UMIs	Urban Morphology Indicators
LMs	Landscape Metrics
NDVI	Normalized Difference Vegetation Index
FAR	Floor Area Ratio
PLAND	Percentage of Landscape Class
AI	Aggregation Index
IJI	Interspersion and Juxtaposition Index
PD	Patch Density
SHDI	Shannon's Diversity Index
OLS	Ordinary Least Squares
SDM	Spatial Durbin Model
VIF	Variance Inflation Factor
AIC	Akaike Information Criterion
BIC	Bayesian Information Criterion

Data availability

Data will be made available on request.

References

Ahmadian, E., Sodagar, B., Bingham, C., Elnokaly, A., & Mills, G. (2021). Effect of urban built form and density on building energy performance in temperate climates. *Energy and Buildings, 236*, Article 110762. https://doi.org/10.1016/j.enbuild.2021.110762

Allen-Dumas, M. R., Rose, A. N., New, J. R., Omitaomu, O. A., Yuan, J., Branstetter, M. L., Sylvester, L. M., Seals, M. B., Carvalhaes, T. M., Adams, M. B., Bhandari, M. S., Shrestha, S. S., Sanyal, J., Berres, A. S., Kolosna, C. P., Fu, K. S., & Kahl, A. C. (2020). Impacts of the morphology of new neighborhoods on microclimate and building energy. *Renewable and Sustainable Energy Reviews, 133*, Article 110030. https://doi.org/10.1016/j.rser.2020.110030

Atikah, N., Rahardjo, S., Afifah, D. L., & Kholifia, N. (2021). Modelling spatial spillovers of regional economic growth in East Java: an empirical analysis based on Spatial Durbin Model. *Journal of Physics: Conference Series, 1872*, Article 012029. https://doi.org/10.1088/1742-6596/1872/1/012029

Bartesaghi-Koc, C., Osmond, P., & Peters, A. (2020). Quantifying the seasonal cooling capacity of 'green infrastructure types' (GITs): An approach to assess and mitigate surface urban heat island in Sydney. *Australia. Landscape and Urban Planning, 203*, Article 103893. https://doi.org/10.1016/j.landurbplan.2020.103893

Beck, H. E., McVicar, T. R., Vergopolan, N., Berg, A., Lutsko, N. J., Dufour, A., Zeng, Z., Jiang, X., van Dijk, A. I. J. M., & Miralles, D. G. (2023). High-resolution (1 km) Köppen-Geiger maps for 1901–2099 based on constrained CMIP6 projections. *Scientific data, 10*, 724. https://doi.org/10.1038/s41597-023-02549-6

Cai, M., Ren, C., Shi, Y., Chen, G., Xie, J., & Ng, E. (2023). Modeling spatiotemporal carbon emissions for two mega-urban regions in China using urban form and panel data analysis. *Science of The Total Environment, 857*, Article 159612. https://doi.org/10.1016/j.scitotenv.2022.159612

Chen, H., Jeanne Huang, J., Li, H., Wei, Y., & Zhu, X. (2023). Revealing the response of urban heat island effect to water body evaporation from main urban and suburb areas. *Journal of Hydrology, 623*, Article 129687. https://doi.org/10.1016/j.jhydrol.2023.129687

Chen, H.-C., Han, Q., & de Vries, B. (2020). Urban morphology indicator analyzes for urban energy modeling. *Sustainable Cities and Society, 52*, Article 101863. https://doi.org/10.1016/j.scs.2019.101863

Chen, Y., Yang, J., Yu, W., Ren, J., Xiao, X., & Xia, J. C. (2023). Relationship between urban spatial form and seasonal land surface temperature under different grid scales. *Sustainable Cities and Society, 89*, Article 104374. https://doi.org/10.1016/j.scs.2022.104374

Costanza, J. K., Riitters, K., Vogt, P., & Wickham, J. (2019). Describing and analyzing landscape patterns: where are we now, and where are we going? *Landscape Ecol, 34*, 2049–2055. https://doi.org/10.1007/s10980-019-00889-6

Cureau, R. J., Pigliautile, I., & Pisello, A. L. (2023). Seasonal and diurnal variability of a water body's effects on the urban microclimate in a coastal city in Italy. *Urban Climate, 49*, Article 101437. https://doi.org/10.1016/j.uclim.2023.101437

DBAG [WWW Document], n.d. URL https://www.3dbag.nl/en/download (accessed 10.9.25).

Dev Roy, S., Kuffer, M., & Wang, J. (2025). Exploring the influence of building morphology on surface temperatures: A multi-city analysis in Europe. *Building and Environment, 282*, Article 113274. https://doi.org/10.1016/j.buildenv.2025.113274

Dijst, M., Worrell, E., Böcker, L., Brunner, P., Davoudi, S., Geertman, S., Harmsen, R., Helbich, M., Holtslag, A. A. M., Kwan, M.-P., Lenz, B., Lyons, G., Mokhtarian, P. L., Newman, P., Perrels, A., Ribeiro, A. P., Rosales Carreón, J., Thomson, G., Urge-Vorsatz, D., & Zeyringer, M. (2018). Exploring urban metabolism—Towards an interdisciplinary perspective. *Resources, Conservation and Recycling, 132*, 190–203. https://doi.org/10.1016/j.resconrec.2017.09.014

Elhorst, J. P. (2014). *Spatial Econometrics: From Cross-Sectional Data to Spatial Panels, SpringerBriefs in Regional Science*. Berlin, Heidelberg: Springer Berlin Heidelberg. https://doi.org/10.1007/978-3-642-40340-8

European Commission. Joint Research Centre. (2024). *JRC-IDEES-2021, the integrated database of the european energy system: data update and technical documentation*. LU: Publications Office. https://doi.org/10.2760/614599.

Frolking, S., Mahtta, R., Milliman, T., Esch, T., & Seto, K. C. (2024). Global urban structural growth shows a profound shift from spreading out to building up. *Nature Cities, 1*, 555–566. https://doi.org/10.1038/s44284-024-00100-1

Ge, J., Wang, Y., Zhou, D., Gu, Z., & Meng, X. (2024). Effects of urban vegetation on microclimate and building energy demand in winter: An evaluation using coupled simulations. *Sustainable Cities and Society, 102*, Article 105199. https://doi.org/10.1016/j.scs.2024.105199

Guo, G., Wu, Z., & Chen, Y. (2019). Complex mechanisms linking land surface temperature to greenspace spatial patterns: Evidence from four southeastern Chinese cities. *Science of The Total Environment, 674*, 77–87. https://doi.org/10.1016/j.scitotenv.2019.03.402

Han, W. (2023). Analyzing the scale dependent effect of urban building morphology on land surface temperature using random forest algorithm. *Scientific Reports, 13*, Article 19312. https://doi.org/10.1038/s41598-023-46437-w

Hou, H., & Estoque, R. C. (2020). Detecting Cooling Effect of Landscape from Composition and Configuration: An Urban Heat Island Study on Hangzhou. *Urban*

Forestry & Urban Greening, 53, Article 126719. https://doi.org/10.1016/j.ufug.2020.126719

Jandaghian, Z., & Colombo, A. (2024). The Role of Water Bodies in Climate Regulation: Insights from Recent Studies on Urban Heat Island Mitigation. *Buildings, 14*, 2945. https://doi.org/10.3390/buildings14092945

Javanroodi, K., Perera, A. T. D., Hong, T., & Nik, V. M. (2023). Designing climate resilient energy systems in complex urban areas considering urban morphology: A technical review. *Advances in Applied Energy, 12*, Article 100155. https://doi.org/10.1016/j.adapen.2023.100155

Jiang, Y., & Huang, Z. (2024). Impact of urban vitality on carbon emission—an analysis of 222 Chinese cities based on the spatial Durbin model. *Humanities & social sciences communications, 11*, 1312. https://doi.org/10.1057/s41599-024-03708-9

Kara, Y., & Yavuz, V. (2025). Urban microclimates in a warming world: Land Surface Temperature (LST) trends across ten major cities on seven continents. *Urban Science, 9*, 115. https://doi.org/10.3390/urbansci9040115

Labetski, A., Vitalis, S., Biljecki, F., Arroyo Ohori, K., & Stoter, J. (2023). 3D building metrics for urban morphology. *International Journal of Geographical Information Science, 37*, 36–67. https://doi.org/10.1080/13658816.2022.2103818

Leng, H., Chen, X., Ma, Y., Wong, N. H., & Ming, T. (2020). Urban morphology and building heating energy consumption: Evidence from Harbin, a severe cold region city. *Energy and Buildings, 224*, Article 110143. https://doi.org/10.1016/j.enbuild.2020.110143

LGN - Basiskaart [WWW Document], n.d. URL https://lgn.nl/basiskaart (accessed 10.9.25).

LeSage, J., & Pace, R. K. (2009). *Introduction to Spatial Econometrics* (0th). Chapman and Hall/CRC. https://doi.org/10.1201/9781420064254.

Li, Y., Ge, J., Wu, H., Tang, R., Cheng, Y., Liu, X., Wang, Y., Zhao, W., Gao, C., Duan, S.-B., Shi, Q., Leng, P., Zhao, E., Yan, G., Song, X., Zhou, C., & Li, Z.-L. (2025). Amplified local cooling effect of forestation in warming Europe. *Nature communications, 16*, 8412. https://doi.org/10.1038/s41467-025-63556-2

Li, Y., Ren, C., Ho, J. Y., & Shi, Y. (2023). Landscape metrics in assessing how the configuration of urban green spaces affects their cooling effect: A systematic review of empirical studies. *Landscape and Urban Planning, 239*, Article 104842. https://doi.org/10.1016/j.landurbplan.2023.104842

Lin, L., Zhao, Y., Zhao, J., & Wang, D. (2025). Comprehensively assessing seasonal variations in the impact of urban greenspace morphology on urban heat island effects: A multidimensional analysis. *Sustainable Cities and Society, 118*, Article 106014. https://doi.org/10.1016/j.scs.2024.106014

Liu, K., Xu, X., Huang, W., Zhang, R., Kong, L., & Wang, X. (2023). A multi-objective optimization framework for designing urban block forms considering daylight, energy consumption, and photovoltaic energy potential. *Building and Environment, 242*, Article 110585. https://doi.org/10.1016/j.buildenv.2023.110585

Liu, Y., Chen, C., Li, J., & Chen, W.-Q. (2020). Characterizing three dimensional (3-D) morphology of residential buildings by landscape metrics. *Landscape Ecol, 35*, 2587–2599. https://doi.org/10.1007/s10980-020-01084-8

Lyu, K., Licina, D., Wienold, J., Tehrani, H. K., & Khovalyg, D. (2024). *A multidomain approach to neighbourhood typology for urban environmental studies*. https://doi.org/10.2139/ssrn.5071013

Mahtta, R., Fragkias, M., Güneralp, B., Mahendra, A., Reba, M., Wentz, E. A., & Seto, K. C. (2022). Urban land expansion: the role of population and economic growth for 300+ cities. *NPJ Urban Sustain, 2*, 5. https://doi.org/10.1038/s42949-022-00048-y

Maps | Natural Capital Atlas [WWW Document], n.d. URL https://www.atlasnatuurlijkkapitaal.nl/kaarten (accessed 10.9.25).

Masoudi, M., & Tan, P. Y. (2019). Multi-year comparison of the effects of spatial pattern of urban green spaces on urban land surface temperature. *Landscape and Urban Planning, 184*, 44–58. https://doi.org/10.1016/j.landurbplan.2018.10.023

National Georegister [WWW Document], n.d. URL https://nationaalgeoregister.nl/geonetwork/srv/dut/catalog.search#/metadata/8dff9ab0-dc82-4143-866f-2c08450abf61 (accessed 12.18.25).

Netherlands, S. (2025). Energy consumption private dwellings; type of dwelling and regions [WWW Document]. *Statistics Netherlands*. URL https://www.cbs.nl/en-gb/figures/detail/81528ENG?utm_source=chatgpt.com accessed 12.9.25.

Oliveira, V. (2020). *Urban Morphology, in: Urban Studies*. Oxford University Press. https://doi.org/10.1093/obo/9780190922481-0004

Overheidspublicaties, n.d. Trees in the Netherlands | Government data [WWW Document]. URL https://data.overheid.nl/dataset/14394-bomen-in-nederland (accessed 2.7.25a).

OverheidspublicatiesOverheidspublicaties, n.d. Low vegetation in the Netherlands | Government data [WWW Document]. URL https://data.overheid.nl/dataset/31026-lage-vegetatie-in-nederland (accessed 10.9.25b).

Qi, J., Xiong, W., Li, J., Zheng, J., Ye, Q., & Hu, M. (2025). Investigating non-linear and synergistic effects of urban functional zone morphology on land surface temperature. *Sustainable Cities and Society, 130*, Article 106546. https://doi.org/10.1016/j.scs.2025.106546

Rapporteer over de duurzaamheid van uw warmtenet [WWW Document], n.d.. RVO.nl. URL https://www.rvo.nl/onderwerpen/verduurzaming-warmtevoorziening/publicaties-warmte-en-koude/rapportage-duurzaamheid (accessed 12.4.25).

Statistiek, C. B.voor de (2025a). *Kerncijfers wijken en buurten 2022 [WWW Document]*. Centraal Bureau voor de Statistiek. URL https://www.cbs.nl/nl-nl/maatwerk/2025/13/kerncijfers-wijken-en-buurten-2022 accessed 10.9.25.

Statistiek, C. B.voor de (2025b). *Verschillen tussen huishoudens [WWW Document]*. Centraal Bureau voor de Statistiek. URL https://www.cbs.nl/nl-nl/longread/aanvullende-statistische-diensten/2025/de-energierekening-januari-2025/4-verschillen-tussen-huishoudens?utm_source=chatgpt.com accessed 12.9.25.

Stewart, I. D., & Oke, T. R. (2012). Local Climate Zones for Urban Temperature Studies. *Bulletin of the American Meteorological Society, 93*, 1879–1900. https://doi.org/10.1175/BAMS-D-11-00019.1

The Netherlands - Countries & Regions [WWW Document], n.d.. IEA. URL https://www.iea.org/countries/the-netherlands/efficiency-demand (accessed 2.6.25).

Tsoka, S., Leduc, T., & Rodler, A. (2021). Assessing the effects of urban street trees on building cooling energy needs: The role of foliage density and planting pattern. *Sustainable Cities and Society, 65*, Article 102633. https://doi.org/10.1016/j.scs.2020.102633

Voskamp, I. M., Sutton, N. B., Stremke, S., & Rijnaarts, H. H. M. (2020). A systematic review of factors influencing spatiotemporal variability in urban water and energy consumption. *Journal of Cleaner Production, 256*, Article 120310. https://doi.org/10.1016/j.jclepro.2020.120310

Voskamp, I. M., Visscher, M. N., Vreugdenhil, C., Van Lammeren, R. J. A., & Sutton, N. B. (2021). Spatial, infrastructural and consumer characteristics underlying spatial variability in residential energy and water consumption in Amsterdam. *Sustainable Cities and Society, 72*, Article 102977. https://doi.org/10.1016/j.scs.2021.102977

Wang, C., Li, Z., Su, Y., Zhao, Q., He, X., Wu, Zhirui, Gao, W., & Wu, Ziting (2024). Impact of block morphology on urban thermal environment with the consideration of spatial heterogeneity. *Sustainable Cities and Society, 113*, Article 105622. https://doi.org/10.1016/j.scs.2024.105622

Wang, R., Murayama, Y., Liu, F., Zhang, X., Hou, H., Morimoto, T., & Derdouri, A. (2025). Impact of urban morphology on land surface temperature: A case study of the central Tokyo. *Japan. City and Environment Interactions, 28*, Article 100227. https://doi.org/10.1016/j.cacint.2025.100227

Weather Data Center [WWW Document], n.d. URL https://www.ashrae.org/technical-resources/bookstore/weather-data-center (accessed 12.9.25).

Wu, H., Zeng, Q., Chen, Q., & Dewancker, B. (2025). Impact of newly constructed parks on urban thermal environment: A comparative analysis of 20 parks before-and-after construction. *Journal of Environmental Management, 373*, Article 123548. https://doi.org/10.1016/j.jenvman.2024.123548

Xi, C., Wang, D., & Cao, S.-J. (2023). Impacts of trees-grass area ratio on thermal environment, energy saving, and carbon benefits. *Urban Climate, 47*, Article 101393. https://doi.org/10.1016/j.uclim.2022.101393

Yang, G., Yu, Z., Jørgensen, G., & Vejre, H. (2020). How can urban blue-green space be planned for climate adaption in high-latitude cities? A seasonal perspective. *Sustainable Cities and Society, 53*, Article 101932. https://doi.org/10.1016/j.scs.2019.101932

Yang, M., Ren, C., Wang, H., Wang, J., Feng, Z., Kumar, P., Haghighat, F., & Cao, S.-J. (2024). Mitigating urban heat island through neighboring rural land cover. *Nature Cities, 1*, 522–532. https://doi.org/10.1038/s44284-024-00091-z

Yang, M., Ye, P., & He, J. (2025). Green and blue infrastructure for urban cooling: Multi-scale mechanisms, spatial optimization, and methodological integration. *Sustainable Cities and Society, 129*, Article 106501. https://doi.org/10.1016/j.scs.2025.106501

Yu, Z., Yang, G., Zuo, S., Jørgensen, G., Koga, M., & Vejre, H. (2020). Critical review on the cooling effect of urban blue-green space: A threshold-size perspective. *Urban Forestry & Urban Greening, 49*, Article 126630. https://doi.org/10.1016/j.ufug.2020.126630

Zhang, J., Ballas, D., & Liu, X. (2023). Neighbourhood-level spatial determinants of residential solar photovoltaic adoption in the Netherlands. *Renewable Energy, 206*, 1239–1248. https://doi.org/10.1016/j.renene.2023.02.118

Zhao, C., & Wang, B. (2022). How does new-type urbanization affect air pollution? Empirical evidence based on spatial spillover effect and spatial Durbin model. *Environment International, 165*, Article 107304. https://doi.org/10.1016/j.envint.2022.107304

Zheng, Y., Ren, C., Xu, Y., Wang, R., Ho, J., Lau, K., & Ng, E. (2018). GIS-based mapping of Local Climate Zone in the high-density city of Hong Kong. *Urban Climate, 24*, 419–448. https://doi.org/10.1016/j.uclim.2017.05.008

Zhou, J., Li, J., Xie, J., Dong, X., Wang, K., Jing, R., Tang, R., & Wang, M. (2025). State-of-the-art review of urban building energy modelling on supporting sustainable development goals. *Applied Energy, 402*, Article 126924. https://doi.org/10.1016/j.apenergy.2025.126924

Zhou, W., Wu, T., & Tao, X. (2024). Exploring the spatial and seasonal heterogeneity of cooling effect of an urban river on a landscape scale. *Scientific Reports, 14*, 8327. https://doi.org/10.1038/s41598-024-58879-x

Zhou, W., Yu, W., & Wu, T. (2022). An alternative method of developing landscape strategies for urban cooling: A threshold-based perspective. *Landscape and Urban Planning, 225*, Article 104449. https://doi.org/10.1016/j.landurbplan.2022.104449

Zhou, X., Huang, Z., Scheuer, B., Wang, H., Zhou, G., & Liu, Y. (2023). High-resolution estimation of building energy consumption at the city level. *Energy, 275*, Article 127476. https://doi.org/10.1016/j.energy.2023.127476

Zhu, S., Causone, F., Gao, N., Ye, Y., Jin, X., Zhou, X., & Shi, X. (2023). Numerical simulation to assess the impact of urban green infrastructure on building energy use: A review. *Building and Environment, 228*, Article 109832. https://doi.org/10.1016/j.buildenv.2022.109832

Zhu, S., Li, Y., Wei, S., Wang, C., Zhang, X., Jin, X., Zhou, X., & Shi, X. (2022a). The impact of urban vegetation morphology on urban building energy consumption during summer and winter seasons in Nanjing, China. *Landscape and Urban Planning, 228*, Article 104576. https://doi.org/10.1016/j.landurbplan.2022.104576

Zhu, S., Yang, Y., Yan, Y., Causone, F., Jin, X., Zhou, X., & Shi, X. (2022b). An evidence-based framework for designing urban green infrastructure morphology to reduce urban building energy use in a hot-humid climate. *Building and Environment, 219*, Article 109181. https://doi.org/10.1016/j.buildenv.2022.109181